Monte Carlo Study of Symmetric Diblock Copolymers in Selective Solvents

Luis A. Molina and Juan J. Freire*

Departamento de Química Física, Facultad de Ciencias Químicas, Universidad Complutense, 28040 Madrid, Spain

Received November 21, 1994; Revised Manuscript Received February 13, 1995[⊗]

ABSTRACT: Systems composed of symmetric copolymer chains in selective solvents have been numerically investigated by means of Monte Carlo simulations in a cubic lattice. Different sets of the reduced attraction energy between nonbonded polymer units of the same type placed in adjacent lattice sites (i.e., of the parameters that describe the solvent quality for each polymer block) have been considered, together with different values of the polymer volume fraction. Configurational properties of the individual chains and their blocks, averaged numbers of unit–unit or unit–solvent contacts, and quantities related with the light scattering of the systems (considering three cases: optical homopolymer, nonrefractive solvent, and isorefractive block) are calculated. All these properties can be used in the characterization of aggregation and ordered microphases (cylindrical microstructures and lamellae). Snapshots of configurations corresponding to representative systems are also shown.

Introduction

The peculiar properties of block copolymer systems have received a great deal of attention in the recent past. Diblock copolymer melts can exhibit microphase separation transitions to form ordered lamellar structures at lower temperatures.[1] Extensive Monte Carlo simulations have been carried out for these systems by different groups using lattice models.[2–7] The same type of transition can be also expected when the copolymers are immersed in a nonselective solvent. Recently,[8] we reported Monte Carlo results for symmetric diblock copolymers in solution, studying the microphase transition as a function of both temperature and concentration. The results for melts and solutions have been discussed in terms of existing mean-field[9] and self-consistent-field[10] theories. In contrast to these theories, a non-Gaussian chain stretch, associated with the transition, has been observed in the simulation data. This stretch, associated with the transition, has been observed in the simulation data. This stretch has been also observed experimentally[11,12] and has been recently interpreted from the theoretical point of view.[13]

However, real solvents cannot be expected to remain nonselective (i.e., of the same thermodynamic quality regarding the different chain blocks) over a broad range of temperatures, except in the case of solvent of very good quality. Therefore, the study of block copolymer solutions should be extended to the more general case of selective solvents, for which micellization is expected to occur at relative low concentrations. The micellization equilibrium in terms of micelle size and proportion of free chains has been the object of a recent simulation work.[14] For higher concentrations, micelles adopt less spherical forms and, eventually, the transition to a nonisotropic ordered phase (as cylindrical structures resulting in hexagonally packed liquid crystals) may take place before the lamellar structure is reached. A similar variety of forms is also found[1,4,15] in nonsymmetric diblock copolymer melts by varying the composition, f (ratio of polymer material in block A to that in block B).

In the present work, we perform a Monte Carlo study of symmetric diblock copolymers in selective solvents of different qualities, over a broad range of concentrations. We obtain global dimensions and other conformational averages of individual chains. Moreover, we evaluate the average number of contacts[6] of different types (A–A, B–B, A–B, A–solvent, and B–solvent) and other averaged properties of the whole system that can be related to light-scattering experiments, as collective form factors, obtained with different sets of contrast factors (proportional to the differences between local refractive indices in the solution sites and the solution mean refractive index). All this variety of properties is then used to characterize the presence of the different types of structures in the solutions. The characterization is confirmed in some representative cases with snapshots of system configurations.

Methods

The chain model employed through this work was detailed in previous papers describing simulation work for homopolymer solutions[16] and symmetric diblock copolymers in nonselective solvents.[8] We place n self-avoiding, monodiperse chains, each of $N = 36$ units, in a simple cubic lattice. Solvent units are associated with the lattice vacancies. In each chain, we distinguish between two blocks, one with $N/2$ units of type A, the other with $N/2$ units of type B ($f = 1/2$). We consider attraction between nonbonded polymer units that are placed in adjacent lattice sites for a given configuration. This attraction is described by the reduced energies ϵ_{AA}/k_BT, ϵ_{BB}/k_BT, and ϵ_{AB}/k_BT, for A–A, B–B, and A–B interactions. Polymer–solvent interactions are not explicitly included. Then, the first two attraction parameters describe the solvent quality (i.e., the balance between the polymer–polymer and polymer–solvent interactions) for the A and B units. We set $\epsilon_{AB}/k_BT = 0$ in all the cases, assuming an effective repulsion between the A and B units. We also define a mean attraction parameter $\bar{\epsilon}/k_BT = (\epsilon_{AA}/k_BT + \epsilon_{BB}/k_BT)/2$. Periodic boundary conditions are introduced in the customary way. The number of chains in the system and the polymer volume (or number of sites) fraction is related by $\phi = nN/L^3$, where L is the box size or cube length. An adequate choice of the box size[3,17] determines the minimum number of chains required to give a reasonably accurate description of the system. In some representative cases, we have carried out the calculation of properties with different values of L, in order to confirm that our lowest choice for L is appropriate for the aims of the present investigation.

Our Monte Carlo algorithm was also previously detailed.[16] We use a combination of local moves, or kink jumps (bents,

[⊗] Abstract published in *Advance ACS Abstracts,* March 15, 1995.

0024-9297/95/2228-2705$09.00/0

crankshafts, and end motions) and reptation motions, according to a conveniently optimized parameter. The Metropolis criterion is used for the acceptance or rejection of new conformations (once the single occupation rule has been enforced). Properties are finally obtained as arithmetic means from the results obtained every 10 Monte Carlo steps or cycles (a Monte Carlo cycle is constituted by nN move attempts). The simulations extend over several tens of thousands of Monte Carlo steps, with a previous thermalization period of (5−10) × 10^3 steps.

Calculation of Properties

(a) Individual Chains. The individual chain size is characterized by the mean quadratic radius of gyration, obtained for every one of the chains included in a given system configuration. It is calculated as

$$\langle R_g^2 \rangle = (1/2N^2)\sum_i^N \sum_j^N (\vec{R}_i - \vec{R}_j)^2 \quad (1)$$

(where $\vec{R}_k$ is the position vector for a chain unit).

We obtained other chain properties, which describe the block behavior within the polymer. These properties have been previously used in theoretical[18,19] and numerical[20] investigations on diblock copolymer chains in dilute systems and in simulations for nonsymmetric[4] and symmetric[7] copolymer melts. We calculate the block mean quadratic radius of gyration

$$\langle R_{g,K}^2 \rangle = (1/2N_K^2)\sum_i^{N_K} \sum_j^{N_K} (\vec{R}_i - \vec{R}_j)^2 \qquad K = A \text{ or } B \quad (2)$$

(the sums extend over the N_K units of the block K) and the mean quadratic distance between the centers of mass of the A and B blocks. For symmetric ($f = 1/2$) chains, this property can be obtained as

$$\langle G^2 \rangle = 4\langle R_g^2 \rangle - 2\langle R_{g,A}^2 \rangle - 2\langle R_{g,B}^2 \rangle \quad (3)$$

Finally, we also compute the mean cosine of the angle formed by vectors $\vec{R}_A$ and $\vec{R}_B$, pointing from the origin to the end of the A and B blocks:

$$\cos\gamma = \langle \cos(\vec{R}_A \wedge \vec{R}_B) \rangle = \langle (R_A^2 + R_B^2 - (\vec{R}_A - \vec{R}_B)^2)/2R_A R_B \rangle \quad (4)$$

(b) Average Number of Contacts. We evaluate the average number of significant interactions, which can help us in the system characterization.[6] Explicitly, we obtain the number of nonbonded unit pairs of a given type, belonging to different chains, or the number of units of a type adjacent to solvent, in a configuration, c_{AA}, c_{AB}, c_{BB}, c_{AS}, and c_{BS} (S represents the solvent). Then we compute the averages

$$r_{AB} = \langle c_{AA}/c_{BB} \rangle \quad (5)$$

$$d_{AB} = \langle c_{AB}/(c_{AA} + c_{BB}) \rangle \quad (6)$$

$$s_K = \langle c_{KS}/2nN(1-\phi) \rangle \qquad K = A, B \quad (7)$$

$$p_K = \langle c_{KK}/nN\phi \rangle \quad (8)$$

and

$$p_{AB} = \langle c_{AB}/2nN\phi \rangle \quad (9)$$

(The denominators in eqs 7−9 are mean-field estimations of these interactions, neglecting intramolecular interactions and end effects.)

(c) Scattering Properties. The collective scattering function of the system can be obtained (in reduced units) as

$$S_{col}(q) = L^{-3}\langle [\sum_i^{L^3} f_i \cos(\vec{q}\cdot\vec{R}_i)]^2 + [\sum_i^{L^3} f_i \sin(\vec{q}\cdot\vec{R}_i)]^2 \rangle \quad (10)$$

where f_i represents a contrast factor proportional to the local fluctuation for the refractive index of site i. The condition

$$q_j = (2\pi/L)k_j \qquad k_j = 0, 1, 2, \ldots \quad (11)$$

applies to the three components ($j = x$, y, or z) of the scattering vector $\vec{q}$. Practically, we are interested in some sets of contrast factors that are able to provide important information on the system structure.

(c1) Optical Homopolymer. Setting

$$f_i = -\phi \qquad \text{if site } i \text{ is solvent}$$

and

$$f_i = (1-\phi) \qquad \text{otherwise} \quad (12)$$

in eq 10, we have obtained $S_{homo}(q)$, the scattering function corresponding to a chain where both blocks have the same refractive index. This function allows us to characterize a macroscopic phase transition (solvent segregation). Thus, according to the random phase approximation theory,[21] the spinodal condition for phase separation is given by

$$\lim_{q\to 0} S_{homo}^{-1}(q) = 0 \quad (13)$$

Then, extrapolations to this limit (also based in the random phase approximation predictions) are performed,[22] and negative values of $S_{homo}^{-1}(0)$ are associated with solvent segregation.

(c2) Nonrefractive Solvent. In this case we set

$$f_i = -1 \qquad \text{if } i \text{ is occupied by an A unit}$$

$$f_i = 0 \qquad \text{if } i \text{ is occupied by solvent}$$

$$f_i = 1 \qquad \text{if } i \text{ is occupied by a B unit} \quad (14)$$

These values, when introduced in eq 10, yield the scattering function $S_{copo}(q)$, similar to the one needed to study copolymer melts. It can be fitted[3,8,9] to

$$S_{copo}^{-1}(q) = (1/N\alpha)[F(q\tilde{R}_g) = \delta] \quad (15)$$

where α, δ, and $\tilde{R}_g$ are fitting parameters and $F(x)$ is the copolymer form factor

$$F(x) = (x^4/2)[(x^2/4) + e^{-x^2/2} - (1/4)e^{-x^2} - (3/4)]^{-1} \quad (16)$$

which has a maximum at $x^* = 1.95$ or $q^* = 1.95/\tilde{R}_g$. The divergence of $S_{copo}(q^*)$ has been previously used to characterize transitions to ordered microphase structures.[9]

$S_{copo}(q)$ can be considered as a fictitious mass distribution in the q space.[3] For a given configuration, we can calculate a "moment-of-inertia" tensor, **T**, consistent

with this distribution. The eigenvalues I_i, and the eigenvectors, $\vec{T}_i$, ($i = 1-3$) of **T**, can be also computed. Then, the quantities[3]

$$Q_1 = (I_3/I_1) + (I_2/I_1) - 2 \tag{17}$$

and

$$Q_2 = (I_3/I_1) - (I_2/I_1) \tag{18}$$

characterize the system anisotropy, together with the principal direction, $\vec{T}_1$ (the normalized eigenvector that corresponds to the smallest eigenvalue). From our Monte Carlo sampling we compute the averages $\langle Q_1 \rangle$ and $\langle Q_2 \rangle$, and the correlation function

$$C_T(\tau) = \langle |\vec{T}_1(t)\cdot\vec{T}_1(t+\tau)| \rangle - {}^1/_2 \tag{19}$$

where t and $t + \tau$ denote given Monte Carlo cycles. Finally, assuming a single "relaxation process",[3] we estimate a normalized "relaxation time" as the value τ_q for which $C_T(q)$ decays to a fraction 1/e of its initial value at $t = 0$.[8] Nonisotropic microstructures are associated with high values of $S_{copo}(q)$ in its peak, high values of τ, and high values of $\langle Q_1 \rangle$.

(c3) Isorefractive Block. We can also set the same contrast factor for one of the blocks and the solvent, and calculate from eq 10 the resulting scattering function, $S_K(q)$ (K = A or B, is the block with different refractive index). In this case, for our symmetric ($f = {}^1/_2$) chains, we have

$$f_i = 1 - \phi/2 \quad \text{if } i \text{ is occupied by block K}$$

$$f_i = -\phi/2 \quad \text{otherwise} \tag{20}$$

This way, we are able to detect the formation of core structures with units of a given type K (micelles or cylinders) for which we expect a divergence (or a negative extrapolated value) for $S_K(0)$. Both $S_A(0)$ and $S_B(0)$ may diverge for lamellar structures.

Numerical Results

In Table 1, we present the results obtained for the conformational properties of individual chains. Table 2 contains the averages of intermolecular interactions (number of contacts). Table 3 shows the values of the different quantities related to light-scattering properties. The analysis of these data should take into account the particular sets of parameters chosen for the different systems. Figure 1 contains a summary of some properties for one of these sets of systems.

(a) Nonselective Systems in the Homopolymer Θ Region. As a reference for more complex systems, we report first our numerical results for the set of parameters $\epsilon_{AA}/k_BT = \epsilon_{BB}/k_BT = 0.3$. This value is close to the Θ point of an individual homopolymer chain.[16] Values of the global radius of gyration for these systems have been previously reported in our previous work on copolymers in nonselective solvents,[8] with slightly poorer statistics. The only significant difference between those earlier results and the present data corresponds to the most concentrated system, $\phi = 0.75$, for which we find now a higher value of $\langle R_g^2 \rangle$. This concentrated system shows a clear lamellar structure (according to our previous findings it is beyond the microphase separation transition,[8] and this conclusion is fully confirmed from the rest of properties that will be analyzed immediately below). Then, the increase of

Table 1. Averaged Quadratic Radius of Gyration of the Chains and Their Blocks, Mean Quadratic Distance between the Center of Mass of the Blocks, and Average Angle between the blocks Origin-to-End Vectors for Systems of Different Solvent Qualities and Concentrations[a]

ϵ_{AA}/k_BT	ϵ_{BB}/k_BT	ϕ	$\langle R_g^2 \rangle$	$\langle R_{g,A}^2 \rangle$	$\langle R_{g,B}^2 \rangle$	$\langle G^2 \rangle$	γ	σ_G
0.3	0.3	0.11	10.35	4.42	4.45	23.7	95.6	1.23
		0.22	10.40	4.41	4.42	23.93	96.0	1.24
		0.26	10.46	4.43	4.42	24.1	95.8	1.25
		0.38	10.33	4.35	4.35	23.9	96.6	1.24
		0.51	10.72	4.35	4.36	25.5	98.8	1.32
		0.75	11.22	4.36	4.38	27.4	101.5	1.42
0.2	0.4	0.037	10.45	4.72	4.20	24.0	95.4	
		0.11	10.39	4.71	4.19	23.8	95.6	
		0.22	10.40	4.65	4.17	24.0	96.2	
		0.26	10.45	4.60	4.19	24.2	96.4	
		0.38	10.67	4.57	4.22	25.1	98.1	
		0.38[b]	10.53	4.53	4.21	24.7	96	
		0.44	10.71	4.52	4.22	25.4	98.8	
		0.51	10.84	4.49	4.22	25.9	99.5	
		0.75	11.02	4.37	4.26	26.8	101.8	
0.0	0.6	0.037	10.16	5.19	3.59	23.2	95.3	
		0.073	10.80	5.17	3.68	25.5	98.2	
		0.11	11.1	5.19	3.81	26.5	99.3	
		0.18	11.73	5.16	3.99	28.6	101.4	
		0.18[c]	11.88	5.17	4.00	29.2	102.1	
		0.22	12.10	5.16	4.07	29.9	103.3	
		0.26	11.80	5.09	4.07	28.9	102.1	
		0.38	12.01	4.98	4.17	29.7	102.6	
		0.38[b]	12.18	5.00	4.21	30.3	103.3	
		0.44	12.25	4.96	4.22	30.7	104.1	
		0.51	12.64	4.97	4.26	32.1	106.8	
		0.62	12.37	4.81	4.28	31.3	105.4	
		0.75	12.13	4.58	4.33	30.3	105.5	
0.275	0.6	0.037	9.74	4.51	3.63	22.7	97.2	
		0.073	9.94	4.59	3.66	23.4	97.9	
		0.11	10.50	4.57	3.87	25.3	99.9	
		0.11[d]	10.58	4.55	3.84	25.5	99.6	
		0.15	10.84	4.60	3.89	26.4	101.0	
		0.15[b]	11.01	4.59	3.87	26.9	101.1	
		0.18	11.4	4.69	4.02	28.3	102.2	
		0.22	11.11	4.59	3.97	27.3	102.3	
		0.38	11.56	4.56	4.16	28.8	103.2	
		0.51	12.53	4.70	4.37	32.0	105.6	
		0.75	12.56	4.56	4.43	32.3	106.3	
0.2	0.8	0.26	11.6	4.78	3.85	29.0	103.9	
		0.38	11.63	4.67	4.03	29.1	103.9	
		0.51	12.33	4.73	4.19	31.5	106.0	
0.275	0.9	0.38	11.63	4.68	3.99	29.2	104.6	
		0.51	11.70	4.51	4.10	29.6	104.5	

[a] The length unit is the separation between adjacent lattice sites. [b] L (box size) = 20. [c] L = 26. [d] L = 30.

dimensions is consistent with a stretch of the chains associated with the microphase formation. For diluted systems, the values of this property do not show any important variation with concentration. However, a small change increase can be noticed for $\phi = 0.51$, in the transition region (pretransitional stretching[13]). For low or moderate concentrations, the data are increased with respect to the radius of gyration of a single homopolymer chain of the same molecular weight,[16] $\langle R_g^2 \rangle_{homo}$, in a factor $\langle R_g^2 \rangle / \langle R_g^2 \rangle_{homo} \cong 1.15$, when $\epsilon/k_BT = 0.3$. As we have previously discussed,[8] this ratio is close to the theoretical predictions of the renormalization group theory,[18,19] and to those obtained from simulation data for longer individual chains.[20] As expected for a nonselective solvent $\langle R_{g,A}^2 \rangle \cong \langle R_{g,B}^2 \rangle$. It is interesting to notice that both averages are not varying as concentration increases (not even for the systems with lamellar structure). They are slightly smaller than 50% the value corresponding to a $N = 36$ homopolymer chain with $\epsilon/k_BT = 0.3$.[16]

Our values of γ for the dilute or moderately concentrated systems, $\gamma \cong 95°$, are also very close to those

Table 2. Quantities Related with the Averaged Number of A–A, A–B, B–B, A–s, or B–s As Defined in the Text

ϵ_{AA}/k_BT	ϵ_{BB}/k_BT	ϕ	r_{AB}	d_{AB}	s_A	s_B	p_A	p_B	p_{AB}
0.3	0.3	0.11	1.03	0.420	0.4671	0.4683	0.3504	0.3401	0.1447
		0.22	1.00	0.378	0.4887	0.4890	0.4060	0.4059	0.1536
		0.26	0.99	0.375	0.4982	0.4973	0.4113	0.4160	0.1552
		0.38	1.00	0.352	0.5250	0.5242	0.4601	0.4632	0.1530
		0.51	0.997	0.268	0.5541	0.5540	0.5263	0.5277	0.1412
		0.75	0.998	0.207	0.6223	0.6209	0.6266	0.6274	0.1295
0.2	0.4	0.037	0.48	0.36	0.4607	0.4406	0.229	0.471	0.126
		0.11	0.51	0.38	0.4821	0.4502	0.2552	0.504	0.1457
		0.22	0.56	0.357	0.5116	0.4609	0.3027	0.5411	0.1507
		0.26	0.564	0.338	0.5228	0.4627	0.3208	0.5719	0.1487
		0.38	0.626	0.290	0.5609	0.4730	0.3844	0.616	0.1454
		0.38[a]	0.623	0.299	0.5604	0.4746	0.3772	0.6048	0.1468
		0.44	0.647	0.275	0.5830	0.4785	0.4064	0.6279	0.1419
		0.51	0.678	0.243	0.6109	0.4834	0.4451	0.6560	0.1339
		0.75	0.837	0.196	0.7108	0.5242	0.5784	0.6909	0.1247
0.0	0.6	0.037	0.10	0.21	0.4738	0.401	0.148	1.560	0.182
		0.037[c]	0.094	0.197	0.4747	0.4004	0.152	1.630	0.172
		0.073	0.093	0.18	0.4872	0.384	0.153	1.639	0.159
		0.11	0.092	0.15	0.5009	0.354	0.172	1.879	0.156
		0.18	0.118	0.14	0.5314	0.325	0.1977	1.676	0.1323
		0.18[b]	0.121	0.134	0.5249	0.315	0.2132	1.776	0.1340
		0.22	0.136	0.13	0.5462	0.308	0.2213	1.639	0.1231
		0.26	0.160	0.144	0.5631	0.317	0.2263	1.412	0.1181
		0.38	0.239	0.149	0.6261	0.311	0.2799	1.171	0.1081
		0.38[a]	0.229	0.13	0.6204	0.296	0.2807	1.223	0.1131
		0.44	0.276	0.137	0.6601	0.296	0.3128	1.134	0.0992
		0.51	0.344	0.142	0.7025	0.300	0.3564	1.037	0.0988
		0.62	0.461	0.145	0.7747	0.3117	0.4287	0.9298	0.0983
		0.75	0.660	0.162	0.8640	0.327	0.4967	0.7524	0.1014
0.275	0.6	0.037	0.17	0.17	0.4538	0.399	0.288	1.72	0.176
		0.073	0.21	0.168	0.4618	0.382	0.341	1.60	0.164
		0.11	0.21	0.145	0.4682	0.351	0.397	1.92	0.169
		0.15	0.23	0.139	0.4763	0.335	0.415	1.81	0.154
		0.18	0.24	0.120	0.4899	0.321	0.416	1.76	0.1298
		0.22	0.270	0.127	0.4998	0.320	0.413	1.524	0.1234
		0.38	0.387	0.1174	0.5588	0.320	0.4465	1.153	0.0939
		0.51	0.488	0.100	0.6245	0.333	0.4835	0.993	0.0812
		0.75	0.738	0.111	0.7516	0.4022	0.611	0.8272	0.0799
0.2	0.8	0.26	0.187	0.092	0.5354	0.2432	0.342	1.832	0.0997
		0.38	0.269	0.095	0.5913	0.2468	0.374	1.387	0.0839
		0.51	0.381	0.100	0.6602	0.248	0.437	1.148	0.0790
0.275	0.9	0.38	0.307	0.082	0.557	0.201	0.472	1.539	0.081
		0.51	0.416	0.091	0.574	0.247	0.475	1.147	0.0833

[a] $L = 20$. [b] $L = 26$. [c] $L = 30$.

found for simulations of long isolated chains in unperturbed or Θ conditions.[20] Something similar can be observed for $\langle G^2 \rangle$. Thus, we have obtained now the value of this property for a homopolymer chain with $\epsilon/k_BT = 0.3$. The result, $\langle G^2 \rangle = 19.3$, yields a ratio between the dilute copolymer and single hompolymer chains, $\sigma_G \cong 1.24$, close to the theoretical and simulation results for unperturbed single chains.[20] Moreover, γ and $\langle G^2 \rangle$ exhibit an increase for higher concentrations similar to the one discussed above for the ratio of gyration. Consequently, we can also associate these increases with chain stretching in the transition to microphase ordering.

The values of averaged number of interactions of the nonselective solvent systems show, as expected that $r_{AB} \cong 1$, $s_A \cong s_B$ over the whole range of concentrations. d_{AB} and p_{AB} decrease for the highest concentrations, as the lamellar structure is formed to favor a further segregation of the blocks. Finally, s_A and s_B show a significant increase for the most concentrated system. It seems that the chain are more exposed to the solvent in the lamellar structure (perhaps because of the chain stretching).

We can observe that the extrapolated values $S_{homo}^{-1}(0)$ are positive for all these nonselective solvent systems; i.e., solvent segregation does not occur as the systems are close to the homopolymer Θ point, and moreover, the repulsive heterointeractions increase the solvent quality.[8,20] Then, the variation of $S_{homo}^{-1}(0)$ with concentration shows the features analyzed previously for hompolymer chains above the critical temperature,[22] with a minimum at intermediate concentration. $S_{copo}(q^*)$ and τ_q, however, increase strongly for $\phi > 0.5$, clearly indicating the formation of an anisotropic (lamellar) structure.[2-4,8] It should be observed that $\langle Q_1 \rangle$ also increases for the lamellar systems, while not significant variations are found for $\langle Q_2 \rangle$. Finally, we point out that the extrapolated values $S_K^{-1}(0)$ are close to zero or negative for the lamellar systems.

(b) Selective Systems with $\bar{\epsilon}/k_BT = 0.3$. We start the analysis of results for selective solvents, with systems where the interaction parameters for type A and type B units are not very different from those set in the nonselective cases, discussed previously in (a). Thus, we consider $\epsilon_{AA}/k_BT = 0.2$ and $\epsilon_{BB}/k_BT = 0.4$. Therefore the solvent is set to be of better quality for the A units. From the conformational properties for individual chains, we observe an earlier increase (at $\phi = 0.38-0.44$) of $\langle R_g^2 \rangle$, $\langle G^2 \rangle$, and γ with increasing concentration. As expected the A block exhibits greater dimensions, $\langle R_{g,A}^2 \rangle > \langle R_{g,B}^2 \rangle$, though the difference decreases for the most concentrated systems. The averaged numbers of interactions reveal a sharp decrease of r_{AB} with respect to the nonselective solvent

Table 3. Quantities Related with the Different Collective Scattering Functions, as Defined in the Text[a]

ϵ_{AA}/k_BT	ϵ_{BB}/k_BT	ϕ	$S_{homo}^{-1}(0)$	$S_{copo}(q^*)/\phi$	$q^*\langle R_g^2\rangle^{1/2}$	$S_B^{-1}(0)$	$S_A^{-1}(0)$	τ_q	$\langle Q_1\rangle$
0.3	0.3	0.11	0.461	10.66	1.93	1.078	1.095	10	0.63
		0.22	0.427	16.43	1.86	0.648	0.495	10	0.59
		0.26	0.445	17.43	1.79	0.410	0.405	20	0.61
		0.38	0.598	26.80	1.65	0.250	0.242	30	0.58
		0.51	0.721	42.79	1.67	0.044	0.043	170	0.68
		0.75	1.894	324.6	1.62	−0.058	−0.013	2820	0.85
0.2	0.4	0.037	1.025	9.80	1.90	2.197	3.024	10	0.65
		0.11	0.496	11.2	1.90	0.696	1.337	10	0.64
		0.22	0.373	15.60	1.83	0.154	0.459	20	0.60
		0.26	0.365	16.72	1.75	−0.015	0.511	20	0.63
		0.38	0.438	34.04	1.65	−0.045	0.396	50	0.61
		0.44	0.481	48.11	1.63	−0.222	0.380	130	0.67
		0.51	0.548	56.71	1.55	−0.158	0.208	160	0.63
		0.75	1.584	65.94	1.45	−0.199	−0.138	>5000	1.44
0.0	0.6	0.037	0.458	10.8	1.92	0.0080	3.680	10	0.72
		0.073	0.376	15.2	1.79	−0.125	2.166	20	0.66
		0.11	0.140	25.6	1.64	−0.237	1.549	30	0.68
		0.18	0.136	52.0	1.58	−0.479	1.195	110	0.69
		0.22	0.117	92.4	1.52	−0.500	0.939	160	0.65
		0.26	0.163	109	1.56	−0.517	0.828	420	0.75
		0.38	0.636	139	1.50	−0.421	0.739	1890	0.78
		0.44	0.781	412	1.59	−0.171	0.202	3110	0.98
		0.51	0.693	396	1.51	−0.427	0.087	>5000	1.29
		0.62	0.741	D	1.66	−0.222	0.111	>5000	1.66
		0.75	0.836	517	1.67	−0.026	−0.036	780	0.95
0.275	0.6	0.037	0.788	11.87	1.85	0.833	3.149	20	0.74
		0.073	0.272	16.35	1.81	−0.454	1.655	30	0.67
		0.11	0.162	27.15	1.61	−0.652	0.819	50	0.70
		0.15	0.033	39.69	1.62	−0.774	0.628	90	0.71
		0.18	0.055	49.18	1.59	−0.611	0.390	180	0.73
		0.22	0.117	50.64	1.55	−0.448	0.358	510	0.81
		0.38	0.163	243.2	1.56	−0.327	0.220	2500	0.91
		0.51	0.216	556.8	1.56	−0.426	0.0723	>5000	1.29
		0.75	0.937	D	1.48	−0.273	−0.175	>5000	1.51
0.2	0.8	0.26	0.171	9.35	1.76	−0.869	0.935	430	0.66
		0.38	0.185	D	1.63	−0.472	0.639	3790	0.63
		0.51	0.113	D	1.54	−0.302	−0.014	>5000	1.49
0.275	0.9	0.38	−0.046	D	1.68	−0.252	0.480	>5000	1.19
		0.51	0.125	D	1.60	−0.441	0.070	>5000	1.95

[a] D indicates divergence of the function.

cases. This decrease is not so much significant for the most concentrated system. d_{AB} and p_{AB} show a behavior close to the nonselective solvent systems, though their decrease is observed to start at lower concentrations. The difference $s_A - s_B$ is small for the dilute systems, but it also changes at moderate concentrations to become significantly higher. It can be observed that s_B does not vary much with increasing concentration, except for the system with $\phi = 0.75$.

From the values of $S_{homo}^{-1}(0)$ we do not observe any indication of solvent segregation ($\bar{\epsilon}/k_BT$ is the same as that in the previously analyzed nonselective solvent systems). $S_{copo}(q^*)$ values have a sharp increase for $\phi = 0.38$ and higher concentrations. The values of $q^*\langle R_g^2\rangle^{1/2}$ contained in Table 3 indicate that a divergence in $S_{copo}(q^*)$ can reflect local anisotropy if it extends over distances that are a few times the radius of gyration. Therefore, these results can correspond to asymmetric micelles. τ_q increases moderately in the same region and shows a very dramatic further increase at higher concentrations, for which global anisotropy can be expected. However, $\langle Q_1\rangle$ only increases for the highest concentration; therefore, it seems that this increase should be associated with global anisotropy. Finally, $S_B^{-1}(0)$ becomes negative for relatively dilute systems, while $S_A^{-1}(0)$ remains clearly positive, except at $\phi = 0.75$. All these features suggest, in our opinion, an early aggregation of chains with micelle formation (for $\phi = 0.26$). These micelles are in equilibrium with single chains.[14] For $\phi \geq 0.38$ we observe a clear anisotropy as the micelles adopt nonsymmetric shapes (ellipsoids). Chain stretching can be, therefore, associated with asymmetric micelles. However, only for the highest concentration we find clear indication of an ordered microphase structure (increase for $\langle Q_1\rangle$). The simultaneous increase in s_B together with the negative value of $S_A^{-1}(0)$ for this system indicates that the microphase does not include cores of a particular type of unit (as those present in ordered structures different from lamellae).

We have also studied systems with $\epsilon_{AA}/k_BT = 0$ and $\epsilon_{BB}/k_BT = 0.6$. Then, the solvent is good for the A units and very poor for the B units (for $\epsilon_{AA}/k_BT = \epsilon_{BB}/k_BT = 0.6$ we have solvent segregation for copolymer chains of the same chain length[8] in nonselective solvents). Some of the properties for these systems are summarized in Figure 1. Chain stretching is noticed even for diluted systems, $\phi = 0.07$, though in the most diluted case the dimensions are smaller than in the previously analyzed cases. For this dilute case, the B block is collapsed to a very compact form, as is revealed from the values of $\langle R_{g,B}^2\rangle$. The dimensions of the B block increase when this block is included in a micelle or microstructure where its properties are expected to correspond to the melt state. (This increase contributes to higher global dimensions, but its effect is clearly differentiated from stretching, which, as discussed in preceding paragraphs, is also characterized by the increase of other properties.) The average number of interactions confirms very different behaviors for the A and B units. The interactions of B units with solvent initially decrease with concentration (as further interchain aggregations tend to avoid these contacts) to

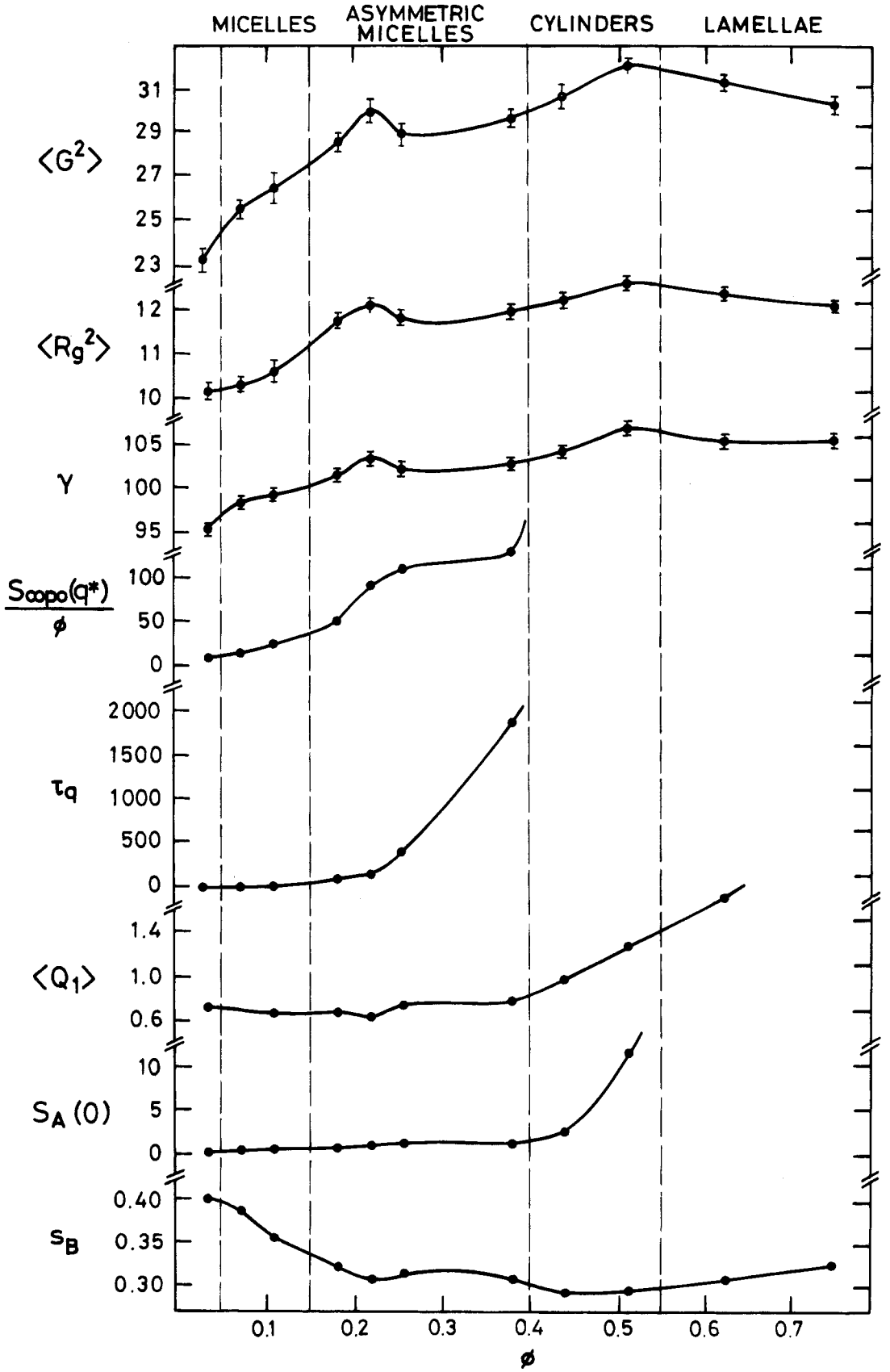

Figure 1. Behavior of different properties versus ϕ for the system $\epsilon_{AA}/k_BT = 0.0$, $\epsilon_{BB}/k_BT = 0.6$ ($N = 36$). Changes associated with transitions are marked by vertical lines.

reach a constant value that indicates the presence of cores. However, the A contacts with solvent are favored as concentration increases (together with the chain stretching). The values of $S_{homo}^{-1}(0)$ indicate that there is not solvent segregation at any concentration. $S_{copo}(q^*)$ reaches high values at $\phi = 0.18$. As we have discussed above, this can be associated with an important local anisotropy. τ_q also increases at $\phi = 0.18$, and becomes very high at $\phi = 0.38-0.44$. $\langle Q_1 \rangle$ shows a noticeable increase only for $\phi = 0.44$. Again, the highest

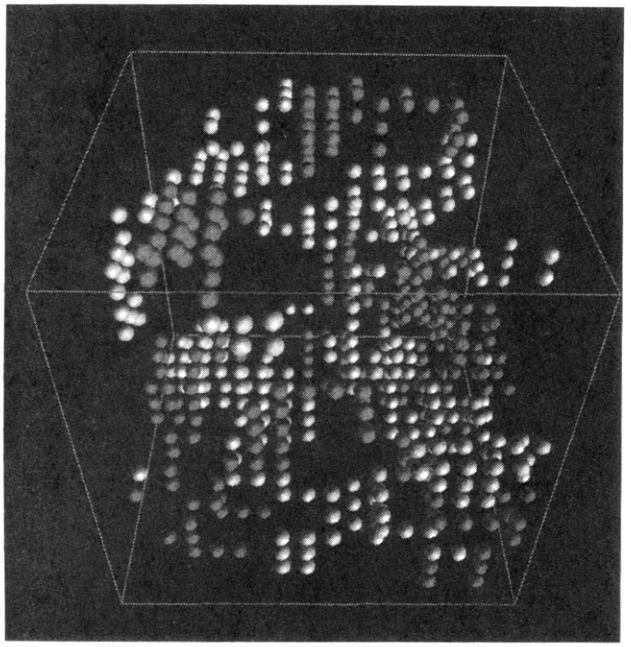

Figure 2. Snapshot of a configuration for the system with $\epsilon_{AA}/k_BT = 0.2$, $\epsilon_{BB}/k_BT = 0.4$, and $\phi = 0.11$ ($N = 36$): (A units) white; (B units) dark.

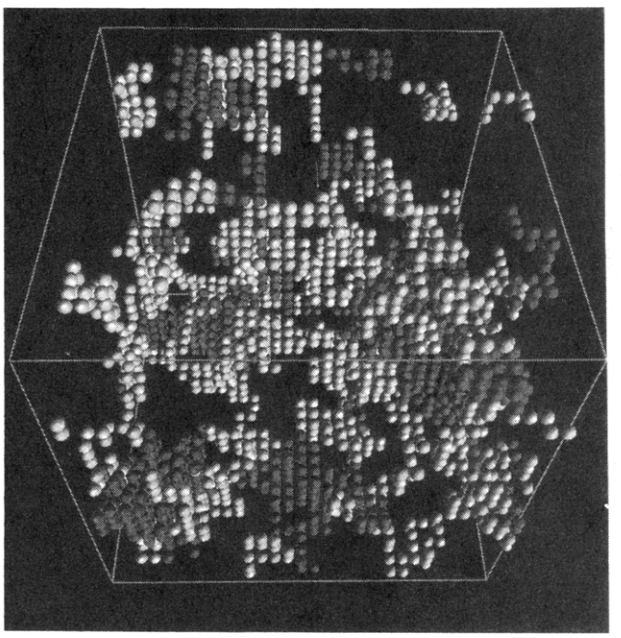

Figure 3. Snapshot of a configuration for the system with $\epsilon_{AA}/k_BT = 0.275$, $\epsilon_{BB}/k_BT = 0.6$, and $\phi = 0.11$ ($N = 36$). Unit codes as in Figure 2.

values of this average are more clearly associated with global anisotropy. $S_B^{-1}(0)$ becomes negative for $\phi = 0.07$, but $S_A^{-1}(0)$ is always positive except for the highest concentration. These data show the formation of micelles for relatively dilute systems, $\phi = 0.07$; these micelles become asymmetric for $\phi = 0.18$. The increase of $\langle Q_1 \rangle$ at $\phi = 0.44$ suggests the transition to an ordered microphase of cylindrical structures. The presence of cores of B units, indicated by a constant s_B and positive values of $S_A^{-1}(0)$, is not compatible with lamellae, for the range of concentrations up to $\phi = 0.51$, but the highest concentration (corresponding to $\phi = 0.75$) data are indicative of a lamellar structure.

(c) Other Selective Solvents. The systems with $\epsilon_{AA}/k_BT = 0.275$, $\epsilon_{BB}/k_BT = 0.6$, i.e., a Θ solvent for the A units and a poor solvent for the B units, show micelle formation at concentrations similar to those of the last case studied in (b) (our reference for these systems) according to the negative values of $S_B^{-1}(0)$, in spite of the lower difference in the solvent quality for the two blocks. (It should be considered that the dimensions are smaller, due to the highest value of $\bar{\epsilon}/k_BT$). Solvent segregation is not observed, though the values of $S_{homo}^{-1}(0)$ at some concentrations are closer to zero. The transition to an ordered structure with cylindrical microstructures is also characterized as a increase of $\langle Q_1 \rangle$, found at lower concentrations. As in the previously analyzed systems, a slight increase in s_B and a value of $S_A^{-1}(0)$ close to zero for the highest concentration may indicate the formation of the lamellar structures.

We have studied some other cases, though only for selected values of concentration. Particularly, we have investigated systems with higher values of $\bar{\epsilon}/k_BT$ in order to investigate the presence of solvent segregation. For $\epsilon_{AA}/k_BT = 0.2$, $\epsilon_{BB}/k_BT = 0.8$ ($\bar{\epsilon}/k_BT = 0.5$), we cannot detect this feature, in contrast with the results obtained[8] for nonselective solvent systems with the same chain length and $\epsilon_{AA}/k_BT = \epsilon_{BB}/k_BT = 0.5$. Micelle formation is found in the region of concentrations for which the solvent segregation was expected to occur, $\phi = 0.22$–0.52. Therefore, it seems that micellar chain aggregation inhibits the macroscopic phase separation. Higher

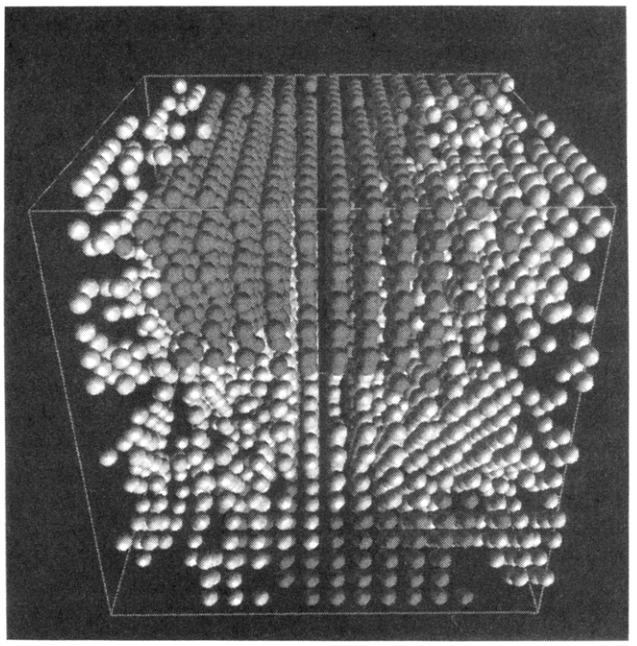

Figure 4. Snapshot of a configuration for the system with $\epsilon_{AA}/k_BT = 0.2$, $\epsilon_{BB}/k_BT = 0.8$, and $\phi = 0.51$ ($N = 36$). Unit codes as in Figure 2.

values of $\langle Q_1 \rangle$, associated to cylindrical structures, are found as in the previously analyzed systems with $\epsilon_{BB}/k_BT = 0.6$. Finally, we have detected solvent segregation for the system $\epsilon_{AA}/k_BT = 0.275$, $\epsilon_{BB}/k_BT = 0.9$ at $\phi = 0.38$. It should be considered that the accuracy of the results decreases for these systems with high attraction between units, whose thermalization is hard to achieve. Therefore, we believe that detailed quantitative analysis of these particular results would not be more conclusive.

Snapshots

Figures 2–5 show configuration snapshots of configurations[5–7] corresponding to some representative systems. Thus, in Figure 2 we can observe a system

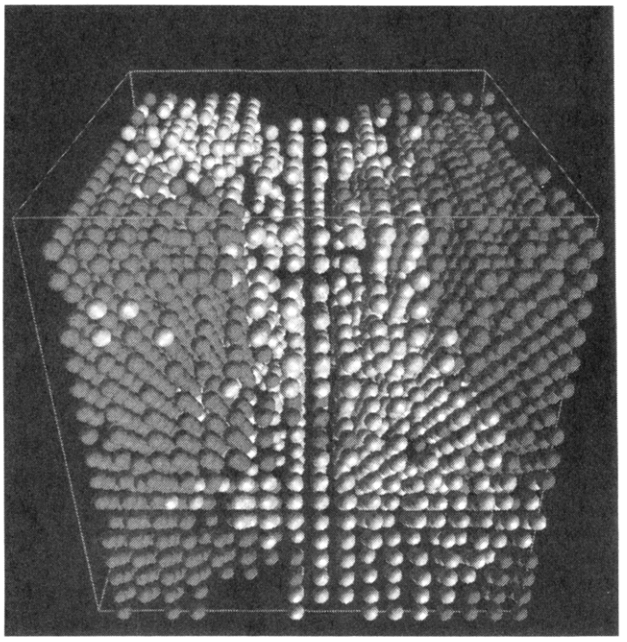

Figure 5. Snapshot of a configuration for the system with $\epsilon_{AA}/k_BT = 0.2$, $\epsilon_{BB}/k_BT = 0.4$ and $\phi = 0.51$ ($N = 36$). Unit codes as in Figure 2.

with only a moderate aggregation of chains. Figure 3 (with a higher box size) contains well-defined micelles coexisting with some free chains. Figure 4 shows an example of cylindrical structure. (The presence of a closed interface crossing the simulation box can be clearly observed). Our box size choice, imposed by practical computational limitations, is not sufficient to characterize the type of packing, associated with the cylindrical microphases. Finally, we present in Figure 5 a system with lamellar structure. (Now, we observe two separate interfaces which extend beyond the simulation box along perpendicular axes). The appearance of all these systems is consistent with the quantitative analysis of properties described in the preceding section.

Concluding Remarks

From the present study, we can confirm the usefulness of Monte Carlo simulations for the study of systems of symmetric diblock copolymer chains in selective solvents. These systems can adopt a variety of aggregation forms and microstructures, depending on the solvent quality for the two blocks and on the polymer concentration. The analysis of numerical results shows consistent patterns which allows us to characterize these features in terms of significant changes for the difference properties (remarked by vertical lines in Figure 1). Thus, the collective scattering function for a nonrefractive solvent is very large or diverges at finite values of the scattering variable in systems with a high degree of anisotropy (local or global). Lamellar structures are associated with the divergence of this function when the solvent is isorefractive with any one of the blocks, while for anisotropic micelles or cylindrical structures we cannot observe this divergence when the solvent is isorefractive with the block included in the cores. Moreover, the average contacts with the solvent, which remain fixed with varying concentration for the units in the cores, increase with increasing concentration for both types of units in the lamellar structures. The transition from anisotropic micelles to cylindrical structures is harder to detect. Tentatively, we associate this transition with a sharp change in the anisotropy of the "tensor-of-inertia" obtained from the distribution of mass in the q space, also calculated from collective scattering functions. We only observe lamellar structure at the highest concentration included in this work ($\phi = 0.75$), at values of $(\bar{\epsilon}/k_BT)\phi$ similar to those found for nonselective solvent systems.[2-8] The cylindrical structures are associated with high differences in the solvent quality with respect to the two blocks. For these systems, a transition to the cylindrical structures is

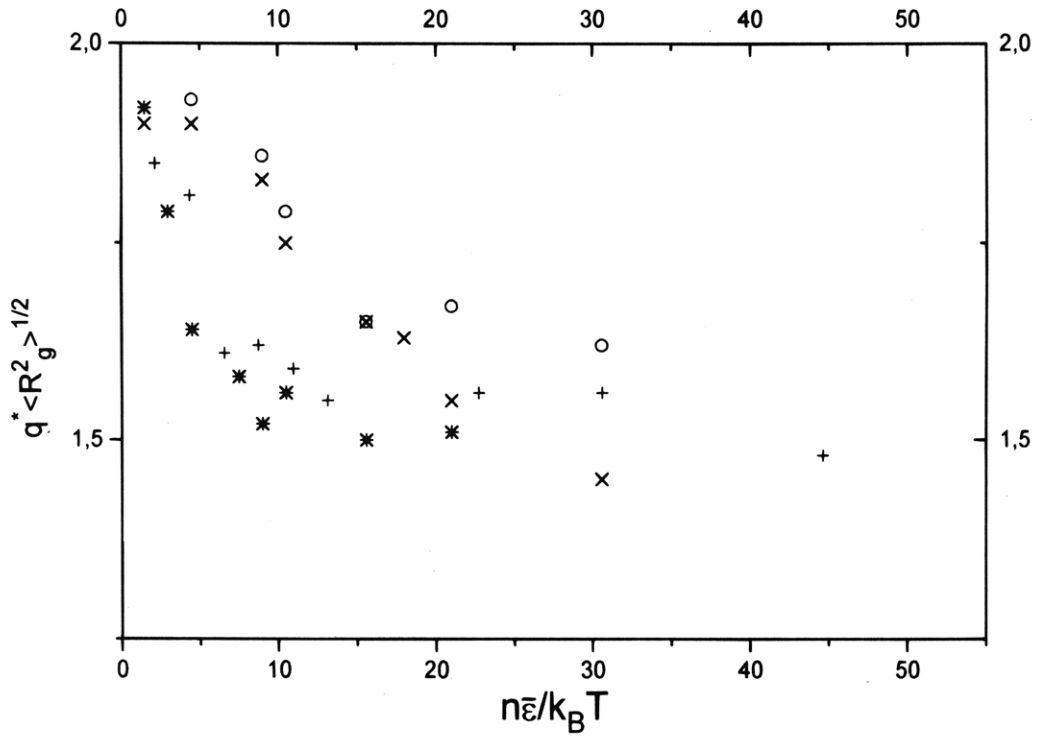

Figure 6. Peak position of $S_{copo}(q)$ versus $(\bar{\epsilon}/k_BT)$ for different systems: (○) system with $\epsilon_{AA}/k_BT = 0.3$ and $\epsilon_{BB}/k_BT = 0.3$; (×) $\epsilon_{AA}/k_BT = 0.2$ and $\epsilon_{BB}/k_BT = 0.4$; (*) $\epsilon_{AA}/k_BT = 0.0$ and $\epsilon_{BB}/k_BT = 0.6$; (+) $\epsilon_{AA}/k_BT = 0.275$ and $\epsilon_{BB}/k_BT = 0.6$. For the present systems $\phi = 7.33 \times 10^{-3}n$.

observed at lower concentrations, as a previous step to the formation of lamellae. Therefore, it seems that the presence of a selective solvent clearly favors the formation of microstructures.

Chain stretching, previously associated with transitions to ordered microphases,[2-4,8,11,12] is now also observed for the different anisotropic aggregation forms or ordered microstructures (anisotropic micelles, cylindrical microstructures, or lamellae). Finally, solvent segregation is only obtained with very high values of the attraction parameters (practically corresponding to low temperatures) since chain aggregation with formation of micelles or microphases competes with macrophase separation. Figure 6 shows fitted values for the peak position of $S_{copo}(q)$ corresponding to different values of a scaling variable proportional to $(\bar{\epsilon}/k_BT)\Phi$. It can be observed that $q^*\tilde{R}_g$ decreases for increasing values of the latter variable. This decrease is faster for the systems with higher $\Delta\epsilon$. For nonselective solvents, however, the previous data[2-4,8] are consistent with a universal behavior.

Acknowledgment. This research was supported by Grant PB92-0227 of the DGICYT (Spain). L. A. Molina acknowledges a fellowship from the PFPI, associated to this Grant.

References and Notes

(1) Bates, F. S.; Fredrickson, G. H. *Ann. Rev. Phys. Chem.* **1990**, *41*, 525.
(2) Minchau, B.; Dünweg, B.; Binder, K. *Polym. Commun.* **1990**, *31*, 348.
(3) Fried, H.; Binder, K. *J. Chem. Phys.* **1991**, *94*, 8349.
(4) Binder, K.; Fried, K. *Macromolecules* **1993**, *26*, 6878.
(5) Haliloğlu, T.; Balaji, R.; Mattice, W. L. *Macromolecules* **1994**, *27*, 1473.
(6) Yang, Y.; Lu, J.; Yan, D.; Ding, J. *Makromol. Chem. Theory Simul.* **1994**, *3*, 731.
(7) Weyersberg, A.; Vilgis, T. A. *Phys. Rev. E* **1993**, *48*, 377.
(8) Molina, L. A.; López Rodriguez, A.; Freire, J. J. *Macromolecules* **1994**, *27*, 1160.
(9) Leibler, L. *Macromolecules* **1980**, *13*, 1602.
(10) Fredrickson, G. H.; Leibler, L. *Macromolecules* **1989**, *22*, 1238.
(11) Hadziioannou, G.; Skoulios, A. *Macromolecules* **1982**, *15*, 258.
(12) Almdal, K.; Rosedale, J. H.; Bates, F. S.; Wignall, G. D.; Fredrickson, G. H. *Phys. Rev. Lett.* **1990**, *65*, 1112.
(13) Tang, H.; Freed, K. F. *J. Chem. Phys.* **1992**, *96*, 8621.
(14) Zhan, Y.; Mattice, W. L. *Macromolecules* **1994**, *27*, 677.
(15) Matsen, M. W.; Schick, M. *Macromolecules* **1994**, *27*, 4014.
(16) López Rodríguez, A.; Freire, J. J. *Macromolecules* **1991**, *24*, 3578.
(17) Kremer, K. *Macromolecules* **1983**, *16*, 1632.
(18) Douglas, J. F.; Freed, K. F. *J. Chem. Phys.* **1987**, *86*, 4280.
(19) Sdrani, Y.; Kosmas, M. K. Macromolecules **1991**, *24*, 1341.
(20) Vlahos, C. H.; Horta, A.; Molina, L. A.; Freire, J. J. *Macromolecules* **1994**, *27*, 2726.
(21) des Cloizeaux, J.; Jennink, G. *Polymers in Solution. Their Modeling and Structure*; Clarendon: Oxford, U.K., 1990.
(22) López Rodríguez, A.; Freire, J. J.; Horta, A. *J. Phys. Chem.* **1992**, *96*, 3954.

MA9460706